#3

Reprinted from ACS SYMPOSIUM SERIES, NO. 198
MECHANISTIC ASPECTS OF INORGANIC REACTIONS
David B. Rorabacher and John F. Endicott, Editors

8

Some Comparisons Between the Energetics of Electrochemical and Homogeneous Electron-Transfer Reactions

MICHAEL J. WEAVER and JOSEPH T. HUPP

Michigan State University, Department of Chemistry, East Lansing, MI 48824

Some conceptual relationships between the kinetics of corresponding electrochemical and homogeneous redox processes are discussed and applied to experimental data for suitable outer-sphere reactions in order to illustrate the utility of electrochemical kinetics for gaining some fundamental insights into the energetics of electron-transfer processes. It is pointed out that electrochemical kinetic and thermodynamic measurements, as a function of temperature and electrode potential, yield direct information on the shapes of the potential-energy surfaces and free energy barriers for individual redox couples. Comparisons between kinetic parameters for corresponding electrochemical and homogeneous exchange reactions show reasonable agreement with the predictions of the conventional "weak overlap" model for several aquo redox couples, but exhibit substantial disagreement for couples containing amines and related ligands. These latter discrepancies may arise from the closer approach of the amine reactants to the electrode surface compared with the strongly solvated aquo complexes. A comparison is also made between the effects of varying the thermodynamic driving force upon the kinetics of related electrochemical and homogeneous reactions. It is shown that the apparent discrepancies seen between the predictions of the harmonic oscillator model and experimental data for some highly exoergic homogeneous reactions may be related to the anomalously small dependence of the rate constant upon overpotential observed for the electrooxidation of aquo complexes. This behavior seems most likely to be due

to a marked asymmetry of the reactant and product free energy barriers for these half reactions.

The kinetics of inorganic electrode reactions have long been the subject of experimental study. The advances in methodology, both in the precise treatment of mass transfer effects and the evolution of electrochemical relaxation techniques, have allowed the kinetics of a wide variety of electrode reactions to be studied. In addition, double-layer structural data are becoming available for a wide range of metal-electrolyte interfaces, which is enabling the kinetics of electrode reactions to be explored quantitatively in a variety of interfacial environments. However, electrode kinetics is a relatively underdeveloped area in comparison with homogeneous redox kinetics, not only in terms of the availability of accurate kinetic data but also in the degree of molecular interpretation.

Nevertheless, simple electrochemical processes of the type

$$Ox + e^- \ (\text{electrode}, \phi_m) \rightleftarrows Red \qquad (1)$$

where both Ox and Red are solution species, form a valuable class of reactions with which to study some fundamental features of electron transfer in condensed media. Such processes involve the activation of only a single redox center, and the free energy driving force can be continuously varied at a given temperature simply by altering the metal-solution potential difference, ϕ_m, by means of an external potential source. In addition, electrode surfaces may exert only a weak electrostatic influence upon the energy state of the reacting species, so that in some cases they could provide a good approximation to the "outer-sphere, weak overlap" limit described by conventional electron-transfer theory. The study of electrochemical kinetics, therefore, provides a unique opportunity to examine separately the reaction energetics of individual redox couples ("half-reactions") which can only be studied in tandem in homogeneous solution. In this paper, some relationships between the kinetics of heterogeneous and homogeneous redox processes are explored in order to illustrate the utility of electrochemical kinetics and thermodynamics for gaining fundamental insights into the energetics of outer-sphere electron transfer.

Electrochemical Rate Formulations

Similar to homogeneous electron-transfer processes, one can consider the observed electrochemical rate constant, k_{ob}, to be related to the electrochemical free energy of reorganization for the elementary electron-transfer step, ΔG^*, by

$$k_{ob} = A \exp(-w_p) \exp(-\Delta G^*/RT) \qquad (2)$$

where A is a frequency factor, and w_p is the work required to transport the reactant from the bulk solution to a site sufficiently close to the electrode surface ("precursor" or "pre-electrode" state) so that thermal reorganization of the appropriate nuclear coordinates can result in electron transfer. Also, for one-electron electroreduction reactions [eq 1] ΔG^* can usefully be separated into "intrinsic" and "thermodynamic" contributions according to (1-3)

$$\Delta G^* = \Delta G^*_{ie} + \alpha[F(E - E^\circ) + w_s - w_p] \qquad (3)$$

where E is the electrode potential at which k_{ob} is measured, E° is the standard (or formal) potential for the redox couple concerned, w_s is the work required to transport the product from the bulk solution to the "successor" state which is formed immediately following electron transfer, α is the (work-corrected) electrochemical transfer coefficient, and ΔG^*_{ie} is the "intrinsic" free energy of activation for electrochemical exchange (3). This last term equals ΔG^* for the particular case when the precursor and successor states have equal energies, i.e., when the free energy driving force for the elementary reaction $[F(E - E^\circ) + w_s - w_p]$ equals zero. The electrochemical transfer coefficient, α, reflects the extent to which ΔG^* is altered when this driving force is nonzero; α therefore provides valuable information on the symmetry properties of the elementary electron-transfer barrier (4).

It is conventional (and useful) to define a "work-corrected" rate constant k_{corr} that is related to k_{ob} at a given electrode potential by

$$k_{corr} = k_{ob} \exp\{[w_p + \alpha(w_s - w_p)]/RT\} \qquad (4)$$

This represents the value of k_{ob} that (hypothetically) would be obtained at the same electrode potential if the work terms w_p and w_s both equalled zero. For outer-sphere reactions, the work terms can be calculated approximately from a knowledge of the average potential on the reaction plane ϕ_{rp}, since $w_p = Z F \phi_{rp}$ and $w_s = (Z - 1)F\phi_{rp}$, where Z is the reactant's charge number. Eq 4 can then be written as

$$k_{corr} = k_{ob} \exp\{[(Z - \alpha)F\phi_{rp}]/RT\} \qquad (5)$$

Usually ϕ_{rp} is identified with the average potential across the diffuse layer ϕ_d^{GC} as calculated from Gouy-Chapman theory using the diffuse-layer charge density obtained from thermodynamic data. In view of the usefulness of k_{corr}, it is also convenient to define a "work-corrected" free energy of activation $\Delta G_e^{\ddagger}$ at a given electrode potential, which is related to k_{corr} by [cf. eq 2]:

$$k_{corr} = A \exp(-\Delta G_e^{\ddagger}/RT) \tag{6}$$

so that eq 3 can be written simply as

$$\Delta G_e^{\ddagger} = \Delta G_{ie}^{\ddagger} + \alpha F(E - E^\circ) \tag{7}$$

Therefore the value of k_{corr} measured at E°, i.e., the "standard" rate constant, k_{corr}^s, is directly related to the intrinsic barrier $\Delta G_{ie}^{\ddagger}$.

In addition, temperature derivatives of k_{corr} can be measured which allows the enthalpic and entropic components of $\Delta G_e^{\ddagger}$ to be obtained. Here an apparent difficulty arises in that a multitude of different Arrhenius plots may be obtained for an electrochemical reaction at a given electrode potential (inevitably measured with respect to some reference electrode), depending upon the manner in which the electrical variable is controlled as the temperature is varied. However, two types of electrochemical activation parameters provide particularly useful information (5-8). The first type, which have been labelled "real" activation parameters ($\Delta H_r^{\ddagger}$, $\Delta S_r^{\ddagger}$) (5, 6), are extracted from an Arrhenius plot of k_{corr}^s as a function of temperature. The significance of these quantities is analogous to that for the activation parameters for homogeneous self-exchange reactions. Thus, $\Delta H_r^{\ddagger}$ equals the activation enthalpy for conditions where the enthalpic driving force, ΔH_{rc}°, for the electrochemical reaction 1 equals zero. Similarly, $\Delta S_r^{\ddagger}$ equals the activation entropy for the (albeit hypothetical) circumstance where the entropic driving force ΔS_{rc}° (the "reaction entropy" (9)) is zero (6). The quantities $\Delta H_r^{\ddagger}$ and $\Delta S_r^{\ddagger}$ are, therefore, equal to the "intrinsic" enthalpic and entropic barriers, $\Delta H_{ie}^{\ddagger}$ and $\Delta S_{ie}^{\ddagger}$, respectively, which together constitute the intrinsic free energy barrier, $\Delta G_{ie}^{\ddagger}$. However, although the activation free energy $\Delta G_e^{\ddagger}$, determined at E°, will equal $\Delta G_{ie}^{\ddagger}$ [eq 7], the enthalpic and entropic barriers at E°, $\Delta H_e^{\ddagger}$ and $\Delta S_e^{\ddagger}$, will differ from $\Delta H_{ie}^{\ddagger}$ and $\Delta S_{ie}^{\ddagger}$. This is because, at E°, generally $\Delta S_{rc}^\circ \neq 0$ (9), and since $\Delta H_{rc}^\circ = T\Delta S_{rc}^\circ$, then also $\Delta H_{rc}^\circ \neq 0$.

Reasonable estimates of $\Delta H_e^{\ddagger}$ and $\Delta S_e^{\ddagger}$ at a given electrode potential can be obtained from an Arrhenius plot measured at the required electrode potential held constant at all temperatures using a "nonisothermal cell" arrangement with the reference electrode compartment maintained at a fixed temperature (8). These quantities, which have been termed "ideal" activation parameters $\Delta H_i^{\ddagger}$ and $\Delta S_i^{\ddagger}$, can be identified with $\Delta H_e^{\ddagger}$ and $\Delta S_e^{\ddagger}$ since the use of such a nonisothermal cell maintains the Galvani metal-solution potential difference, ϕ_m, and, hence, the energy of the reacting electron, essentially constant as the temperature is varied (8, 9).

Similarly, the reaction entropy, ΔS_{rc}°, for a given redox couple can be determined from the temperature derivative of the standard potential, E_{ni}°, measured using a nonisothermal cell, i.e., $\Delta S_{rc}^\circ = F(dE_{ni}^\circ/dT)$, since (dE_{ni}°/dT) should approximately equal the desired temperature dependence of the standard Galvani potential, $(d\phi_m^\circ/dT)$ (9). The reaction entropy provides a useful measure of the changes in the extent of solvent polarization for a single redox couple brought about by electron transfer (9). Since $\Delta G_{rc}^\circ = F(E - E^\circ)$, the corresponding enthalpic driving force, ΔH_{rc}°, for the electrode reaction can be found from $\Delta H_{rc}^\circ = F(E - E^\circ) + T\Delta S_{rc}^\circ$. It is simple to show that the corresponding values of $\Delta H_i^{\ddagger}$ and $\Delta H_r^{\ddagger}$, and $\Delta S_i^{\ddagger}$ and $\Delta S_r^{\ddagger}$ at a given electrode potential are related by (6)

$$\Delta H_i^{\ddagger} = \Delta H_r^{\ddagger} + \alpha T\Delta S_{rc}^\circ \tag{8}$$

and

$$\Delta S_i^{\ddagger} = \Delta S_r^{\ddagger} + \alpha\Delta S_{rc}^\circ \tag{9}$$

Consequently, a wealth of information on the energetics of electron transfer for individual redox couples ("half-reactions") can be extracted from measurements of reversible cell potentials and electrochemical rate constant-overpotential relationships, both studied as a function of temperature. Such electrochemical measurements can, therefore, provide information on the contributions of each redox couple to the energetics of the bimolecular homogeneous reactions which is unobtainable from ordinary chemical thermodynamic and kinetic measurements.

Relationship Between Electrochemical and Homogeneous Reaction Energetics

Consider the following pair of electrochemical reduction and oxidation reactions

$$Ox_1 + e^-(\text{electrode},\phi_m) \rightleftarrows Red_1 \quad (10a)$$

$$Red_2 \rightleftarrows Ox_2 + e^-(\text{electrode},\phi_m) \quad (10b)$$

and the corresponding homogeneous cross reaction

$$Ox_1 + Red_2 \rightleftarrows Red_1 + Ox_2 \quad (11)$$

Providing that the interactions between the reactant and the electrode in the electrochemical transition state, and between the two reactants in the homogeneous transition state, are negligible ("weak overlap" limit), the activation barriers for reactions 10 and 11 will be closely related.

At a given value of ϕ_m (and, hence, electrode potential E), the thermodynamics of reactions 10 and 11 are identical since the energy required to transport the electron across the metal-solution interface in the half reactions 10a and 10b will then cancel. The overall activation free energy, $\Delta G^*_{h,12}$, for reaction 11 can be considered to consist of separate contributions, $\Delta G^*_{h,1}$ and $\Delta G^*_{h,2}$, arising from the activation of Ox and Red, respectively. Although a multitude of different transition-state structures may be formed, corresponding to different individual values of $\Delta G^*_{h,1}$ and $\Delta G^*_{h,2}$, the predominant reaction channel will be that corresponding to a minimum in the activation free energy, $(\Delta G^*_{h,1} + \Delta G^*_{h,2})_{min}$ (10). In the "weak overlap" limit, each pair of values of $\Delta G^*_{h,1}$ and $\Delta G^*_{h,2}$ satisfying the thermodynamic constraints of reaction 11 will be identical to the corresponding pair of electrochemical free energies of activation, $\Delta G^*_{e,1}$ and $\Delta G^*_{e,2}$, for reactions 10a and 10b, respectively, having the same transition-state structures. Therefore the energetics of reactions 10 and 11 are related in the "weak overlap" limit by

$$(\Delta G^*_{e,1} + \Delta G^*_{e,2})^E_{min} = (\Delta G^*_{h,1} + \Delta G^*_{h,2})_{min} = \Delta G^*_{h,12} \quad (12)$$

where $(\Delta G^*_{e,1} + \Delta G^*_{e,2})^E_{min}$ refers to the particular electrode potential where the sum of $\Delta G^*_{e,1}$ and $\Delta G^*_{e,2}$ is a minimum. Only the sum $(\Delta G^*_{h,1} + \Delta G^*_{h,2})_{min}$ can be determined experimentally for a given homogeneous reaction. In contrast, the values of

$\Delta G^*_{e,1}$ and $\Delta G^*_{e,2}$ may be examined individually as a function of the free energy driving forces, ΔG°_1 and ΔG°_2, for these two half reactions, 10a and 10b, which equal $F(E - E^\circ_1)$ and $F(E - E^\circ_2)$, respectively, where E°_1 and E°_2 are the corresponding standard electrode potentials.

This relationship is illustrated schematically in Figure 1. Curves 11' and 22' represent plots of ΔG^*_e against the reaction free energy $F(E - E^\circ)$ for a pair of cathodic and anodic half reactions on a common scale of electrode potential FE; such curves are generally expected to be curved in the manner shown (vide infra) so that a shallow minimum in the plot of $(\Delta G^*_{e,1} + \Delta G^*_{e,2})$ versus FE will be obtained. In practice, unless ΔG^*_e is small ($\lesssim$ 3-4 kcal mol^{-1}), the slopes of these plots, i.e., the cathodic and anodic transfer coefficients, are often to be found to be equal and close to 0.5 so that to a good approximation (11,12)

$$2\Delta G^*_{e,12} = \Delta G^*_{h,12} \quad (13)$$

where $\Delta G^*_{e,12}$ is the value of ΔG^*_e at the intersection of the $(\Delta G^*_{e,1} - E)$ and $(\Delta G^*_{e,2} - E)$ plots. [A previous claim (11) that eq 13 is applicable in the "weak overlap" limit when $\Delta G^*_{e,1}$ and $\Delta G^*_{e,2}$ exhibit a quadratic dependence upon $(E - E^\circ)$ (1) is not entirely correct. The energy minimization condition $\{\partial(\Delta G^*_{e,1} + \Delta G^*_{e,2})/\partial\beta = 0\}$ employed in the appendix of ref. 11 leads to eq 12, eq 13 only being obtained as a special case when the slopes of the $(\Delta G^*_{e,1} - E)$ and $(\Delta G^*_{e,2} - E)$ plots are equal but of opposite sign at the intersection point].

For the special case where the cathodic and anodic half-reactions are identical, since the two plots of $\Delta G^*_e - E$ must intersect at E° for the redox couple, then eq 13 can be written in terms of the electrochemical and homogeneous intrinsic barriers:

$$2\Delta G^*_{ie} = \Delta G^*_{ih} \quad (14)$$

Relationships having the same form as eq 14 can also be written for the enthalpic and entropic contributions to the intrinsic free energy barriers (10). Provided that the reactions are adiabatic and the conventional collision model applies, eq 14 can be written in the familiar form relating the rate constants of electrochemical exchange and homogeneous self-exchange reactions (13):

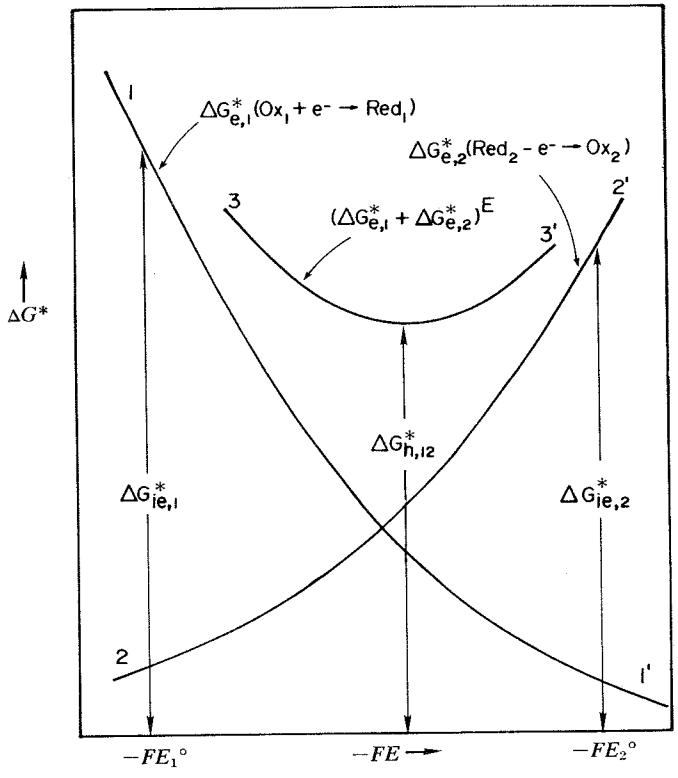

Figure 1. Schematic illustration of the general relationship between electrochemical and homogeneous redox reaction energetics. Curve 1–1′ is a plot of activation free energy, ΔG_e^*, vs. thermodynamic driving force, −FE, for an electroreduction [$\Delta G_{e,1}(Ox_1 + e^- \rightarrow Red_1)$] reaction; and Curve 2–2′ is a plot of ΔG_e^* vs. −FE for an electrooxidation [$\Delta G_{e,2}^*(Red_2 - e^- \rightarrow Ox_2)$] reaction (Reactions 10a and 10b, respectively). E_1° and E_2° are the standard electrode potentials for these two redox couples. Curve 3–3′ is formed by the sum $(\Delta G_{e,1}^* + \Delta G_{e,2}^*)^E$. The corresponding homogeneous activation barrier, $\Delta G_{h,12}^*$, is, in the "weak overlap" limit, given by the minimum in this curve (Eq. 12).

$$\frac{(k_{corr}^{s})^2}{(Z_e)^2} = \frac{k_{corr}^{h,ex}}{Z_h} \qquad (15)$$

where $k_{corr}^{h,ex}$ is the (work-corrected) rate constant for homogeneous self exchange, and Z_e and Z_h are the electrochemical and homogeneous collision frequencies, respectively.

In the following sections, we shall explore the applicability of such relationships to experimental data for some simple outer-sphere reactions involving transition-metal complexes. In keeping with the distinction between intrinsic and thermodynamic barriers [eq 7], exchange reactions will be considered first, followed by a comparison of driving force effects for related electrochemical and homogeneous reactions.

Electron Exchange

Tables I and II contain electrochemical kinetic and related thermodynamic parameters for several transition-metal redox couples gathered at the mercury-aqueous interface. These systems were selected since the kinetics can be measured accurately under experimental conditions where the diffuse-layer potentials, ϕ_d, are small and/or could be estimated with confidence, yielding trustworthy estimates of k_{corr}^{s} from the observed values, k_{ob}^{s} [eq 5]. (Details are given in refs 11 and 14.) Also, the observed rates probably refer to outer-sphere pathways, and the rate constants for the corresponding homogeneous self-exchange reactions are available or can be estimated from rate data for closely related cross reactions (15). These latter values, $k_{corr}^{h,ex}$, which are also corrected for electrostatic work terms (15), are given alongside in Table I for comparison. Also included are estimates of $k_{corr}^{h,ex}$, $k_{corr}^{h,ex}$(calc), that were obtained from the corresponding values of k_{corr}^{s} using eq 15. [Values of 5×10^3 cm s^{-1} and 2×10^{11} M^{-1} s^{-1} were employed for Z_e and Z_h, respectively, appropriate for a "typical" reactant mass of 200 and radius 3.5Å. The estimate of Z_h given in refs 11 and 15 (6×10^{10} M^{-1} s^{-1}) is incorrect due to calculational error.]

It is seen that the values of $k_{corr}^{h,ex}$ for the five aquo couples in Table I are uniformly larger than the corresponding

Table I
Rate Constants and Thermodynamic Parameters for Selected Electrochemical Exchange and Homogeneous Self-Exchange Reactions at 25°C.

Redox Couple	E^f [a]	ΔS°_{rc} [b]	k^s_{corr} [c]	$k^{h,ex}_{corr}$ [d]	$k^{h,ex}_{corr(calc)}$ [e]
	mV vs. s.c.e.	cal deg^{-1} mol^{-1}	cm s^{-1}	M^{-1} s^{-1}	$M^{-1}s^{-1}$
$Ru(OH_2)_6^{3+/2+}$	-15 (0.3)	36	2×10^{-2}	200	3
$V(OH_2)_6^{3+/2+}$	-475 (0.2)	37	1×10^{-3}	3×10^{-2}	8×10^{-3}
$Fe(OH_2)_6^{3+/2+}$	500 (0.2)	43	$\sim 1 \times 10^{-4}$	15	8×10^{-5}
$Eu(OH_2)_n^{3+/2+}$	-625 (0.2)	48	8×10^{-5}	4×10^{-4}	5×10^{-5}
$Cr(OH)_6^{3+/2+}$	-660 (1)	49	2×10^{-6}	2×10^{-6}	3×10^{-8}
$Ru(NH_3)_6^{3+/2+}$	-180 (0.2)	18	$\gtrsim 10$	5×10^{4}	$\gtrsim 8 \times 10^{5}$
$Co(en)_3^{3+/2+}$ [j]	-460 (1)	37	5×10^{-2} [f]	2.5×10^{-4}	20
$Co(bpy)_3^{3+/2+}$ [k]	70 (0.05)	22	$\sim 5 \times 10^{-4}$ [f]	~80	2×10^{-3}
$Co(EDTA)^{-/2-}$	135 (0.5) [i]	-8 [i]	$\sim 5 \times 10^{-2}$ [g]	$\sim 1 \times 10^{-6}$ [h]	20

Notes to Table I

[a] Formal potential of redox couple, determined at ionic strength noted in parentheses. Data from ref. 9 unless otherwise indicated.

[b] Reaction entropy of redox couple, determined at same ionic strength as E^f. Data from ref. 9 unless otherwise indicated.

[c] Standard rate constant for redox couple measured in 0.1-0.4 M KPF_6 and/or $NaClO_4$ supporting electrolytes, corrected for electrostatic double-layer effect using eq. 5 assuming that $\phi_{rp} = \phi_d^{GC}$. Kinetic data from ref. 11 unless otherwise stated.

[d] Rate constant for homogeneous self exchange, corrected for electrostatic work terms using Debye-Hückel-Bronsted model. Data taken from sources quoted in ref. 15 unless otherwise stated.

[e] Rate constant for homogeneous self exchange, calculated from corresponding value of k^s_{corr} using eq. 14, assuming that $Z_e = 5 \times 10^3$ cm s^{-1}, and $Z_h = 2 \times 10^{11}$ M^{-1} s^{-1} (see text).

[f] Sahami, S.; Farmer, J.; Weaver, M. J., unpublished results.

[g] Tanaka, N.; Yamada, A. Electrochim. Acta, 1969, 14, 491.

[h] Quoted in R. G. Wilkins, R. E. Yelin, Inorg. Chem., 1968, 7, 2667.

[i] Yee, E. L.; Weaver, M. J., unpublished results.

[j] en = ethylenediamine.

[k] bpy = 2,2'-bipyridine.

Table II
Comparison between Experimental Reorganization Parameters
for some Electrochemical and Homogeneous Exchange Reactions

Redox Couple	[a] $2\Delta G^{\ddagger}_{ie}$ kcal mol^{-1}	[b] $2\Delta H^{\ddagger}_{ie}$ kcal mol^{-1}	[c] $2\Delta S^{\ddagger}_{ie}$ cal deg^{-1} mol^{-1}	[d] ΔG_{ih} kcal mol^{-1}	[e] $\Delta H^{\ddagger}_{ih}$ kcal mol^{-1}	[f] $\Delta S^{\ddagger}_{ih}$ cal deg^{-1} mol^{-1}
$V(OH_2)_6^{3+/2+}$	18.2	16.5	-5.5	17.5	13.0	-15
$Eu(OH_2)_6^{3+/2+}$	21.2	17.2	-9	20.0	~15.5	(-15)
$Cr(OH_2)_6^{3+/2+}$	25.6	23.4	-7.5	23.2	~18.5	(-15)
$Co(en)_3^{3+/2+}$	13.6	~0 [g]	-45	20.3	13.8	-22

[a] Twice the intrinsic electrochemical free energy of activation, obtained from value of k^{s}_{corr} at mercury-aqueous interface given in Table I using $\Delta G^{\ddagger}_{ie} = -RT \ln(k^{s}_{corr}/Z_e)$, where $Z_e = 5 \times 10^3$ cm s^{-1}.

[b] Twice the intrinsic ("real") electrochemical enthalpy of activation, obtained from $H^{\ddagger}_{ie} = -R[d(\ln k^{s}_{corr} - \ln T^{\frac{1}{2}})/d(1/T)]$ (see text). See refs. 8 and 11 for original data, except where indicated.

[c] Twice the intrinsic ("real") electrochemical entropy of activation, obtained from $2T\Delta S^{\ddagger}_{ie} = 2\Delta H_{ie} - 2\Delta G^{\ddagger}_{ie}$.

[d] Intrinsic free energy of activation for homogeneous self-exchange, obtained from values of $k^{h,ex}_{corr}$ given in Table I using $\Delta G^{\ddagger}_{ih} = -RT \ln(k^{h,ex}_{corr}/Z_h)$, where $Z_h = 2 \times 10^{11}$ M^{-1} s^{-1}.

Notes to Table II Continued.

[e] Intrinsic enthalpy of activation for homogeneous self-exchange. Values for $V^{3+/2+}_{aq}$ and $Co(en)_3^{3+/2+}$ obtained experimentally (see ref. 15 for sources and and calculational details). Values for $Eu^{3+/2+}_{aq}$ and $Cr^{3+/2+}_{aq}$ obtained from $\Delta G^{\ddagger}_{ih}$ assuming that $\Delta S^{\ddagger}_{ih} = -15$ e.u.

[f] Intrinsic entropy of activation for homogeneous self-exchange. Values for $V^{3+/2+}_{aq}$ and $Co(en)_3^{3+/2+}$ obtained from $T\Delta S^{\ddagger}_{ih} = \Delta H^{\ddagger}_{ih} - \Delta G^{\ddagger}_{ih}$. Values in parentheses are estimates, based on the observation that $\Delta S^{\ddagger}_{ih} \simeq -15$ e.u. for several related aquo redox couples (15).

[g] Farmer, J.; Weaver, M. J., unpublished results.

values of $k_{corr}^{h,ex}$(calc) by typically 1-2 orders of magnitude, although the value of $k_{corr}^{h,ex}$ for $Fe_{aq}^{3+/2+}$ (where "aq" denotes aquo ligands) is over 10^5-fold larger than $k_{corr}^{h,ex}$(calc). Such discrepancies have been discussed previously (11). The most general derivation of eq 14 [and hence eq 15] involves the assumption that the stabilization of the electrochemical transition state resulting from the proximity of the reactant to the electrode surface will equal one half of the corresponding stabilization of the homogeneous transition state arising from the approach of the two reactants (13). In terms of the conventional model, this will occur when the distance R^h between the homogeneous reactants equals the distance R^e between the heterogeneous reactant and its electrostatic image in the electrode (13). The observation that $k_{12}^{h,ex} > k_{12}^{h,ex}$(calc), and, hence, $2\Delta G_{ie}^{\ddagger} > \Delta G_{ih}^{\ddagger}$, is expected for electrochemical outer-sphere reactions on this basis since the reactant plus coordinated ligands will be separated from the electrode surface by the "inner layer" of solvent molecules (i.e., the electrode's "coordination layer") so that generally $R^e > R^h$. From the rate responses for Cr_{aq}^{3+} and Eu_{aq}^{3+} reduction at the mercury-aqueous interface to systematic variations in the double-layer structure, it has been concluded that at least two, and possibly three, water molecules lie between the electrode surface and the metal cations in the transition state (16).

Additional insight can be obtained by comparing the electrochemical and homogeneous activation parameters. Table II contains values of $2\Delta G_{ie}^{\ddagger}$, $2\Delta H_{ie}^{\ddagger}$, and $2\Delta S_{ie}^{\ddagger}$ for three aquo couples [$V_{aq}^{3+/2+}$, $Eu_{aq}^{3+/2+}$, and $Cr_{aq}^{3+/2+}$] for which work term corrections can be reliably made as a function of temperature (8). The values of $\Delta G_{ie}^{\ddagger}$ were obtained from the corresponding values of k_{corr}^{s} using eq 6, assuming that the frequency factor A equals Z_e (5×10^3 cm s^{-1}). The intrinsic enthalpies of activation $\Delta H_{ie}^{\ddagger}$ were obtained from the slope of a plot of $-R(\ln k_{corr}^{s} - \ln T^{\frac{1}{2}})$ versus 1/T (8) and the corresponding intrinsic entropies of activation $\Delta S_{ie}^{\ddagger}$ from $\Delta S_{ie}^{\ddagger} = (\Delta H_{ie}^{\ddagger} - \Delta G_{ie}^{\ddagger})/T$. Table II also contains the intrinsic free energies ($\Delta G_{ih}^{\ddagger}$), enthalpies ($\Delta H_{ih}^{\ddagger}$), and entropies of activation ($\Delta S_{ih}^{\ddagger}$) for the corresponding homogeneous self-exchange reactions. These were similarly obtained from the work-corrected homogeneous rate constants. (See ref 15 for calculational details and data sources.)

Comparison of the corresponding electrochemical and homogeneous reorganization parameters reveal that $2\Delta G_{ie}^{\ddagger} > \Delta G_{ih}^{\ddagger}$, which follows from the observation that $k_{corr}^{h,ex} > k_{corr}^{h,ex}$(calc) [eq 14]. This inequality in free energies is paralleled by greater differences between $2\Delta H_{ie}^{\ddagger}$ and $\Delta H_{ih}^{\ddagger}$, these being partially compensated by values of $2\Delta S_{ie}^{\ddagger}$ that are significantly less negative than $\Delta S_{ih}^{\ddagger}$. The classical model of outer-sphere electron transfer predicts that both $\Delta S_{ie}^{\ddagger}$ and $\Delta S_{ih}^{\ddagger}$ should be close to zero (within ca. 1 eu) (11,17). Part, but probably not all, of the observed negative values of $\Delta S_{ie}^{\ddagger}$ can be ascribed to the influence of nuclear tunneling and nonadiabaticity (17); these factors may account entirely for the observed small negative values of $\Delta S_{ie}^{\ddagger}$. The larger negative values of $\Delta S_{ih}^{\ddagger}$ may arise partly from the solvent ordering that probably attends the formation of the highly charged precursor complex from the separated cationic reactants (15). Nevertheless, by and large the relative values of the electrochemical and homogeneous reorganization parameters are reasonably close to the expectations of the weak overlap model (13). The observed differences are consistent with the anticipated smaller extent of the reactant-electrode interactions as compared with the homogeneous reactant-reactant interactions in the transition states for electron transfer.

The remaining four redox couples in Table I, containing amine and related ligands, exhibit values of $k_{corr}^{h,ex}$ that are very different from the corresponding electrochemical estimates $k_{corr}^{h,ex}$(calc). Similar discrepancies between the experimental results and the predictions of eq 15 have been observed previously (18-20), although corrections for work terms have seldom been made. A puzzling feature of these data is the relatively small variation in k_{corr}^{s} and hence $k_{corr}^{h,ex}$(calc) for the three Co(III)/(II) couples compared with $k_{corr}^{h,ex}$. These discrepancies may arise from differences in electronic transmission coefficients at the electrode surface and in the bulk solution (18), from additional contributions to the work terms not considered in the Debye-Hückel and/or Gouy-Chapman models, or from unexpected differences in the outer-shell reorganization energies in the surface and bulk environments (11).

Electrochemical and homogeneous reorganization parameters for $Co(en)_3^{3+/2+}$ are also given in Table II. The large disparity between the electrochemical and homogenous parameters is high-

lighted by a value of $\Delta H^{\ddagger}_{ie}$ that is close to zero. Since the inner-shell contribution to $\Delta H^{\ddagger}_{ie}$ is undoubtedly large ($\gtrsim$5 kcal mol^{-1}), this result indicates that the electrode is markedly influencing the transition-state structure. We have also obtained comparable electrochemical reorganization parameters for the $Co(NH_3)_6^{3+/2+}$ couple. Since there is strong evidence that ammine complexes can approach the electrode surface more closely than the more strongly solvated aquo complexes (16), it seems likely that this unexpected electrochemical behavior of $Co(en)_3^{3+/2+}$ arises from a specific influence of the interfacial environment.

Influence of the Thermodynamic Driving Force

Given that the reorganization parameters for electrochemical exchange of various aquo redox couples are in acceptable agreement with the corresponding homogeneous rate parameters on the basis of the weak overlap model, it is of interest to compare the manner in which the energetics of these two types of redox processes respond to the application of a net thermodynamic driving force.

For one-electron electrochemical reactions, the harmonic oscillator ("Marcus") model (21) yields the following predicted dependence of $\Delta G^{\ddagger}_e$ upon the electrode potential:

$$\Delta G^{\ddagger}_e = \Delta G^{\ddagger}_{ie} \pm 0.5\ F(E - E^\circ) + \frac{F(E - E^\circ)^2}{16\Delta G^{\ddagger}_{ie}} \qquad (16)$$

where the plus/minus sign refers to reduction and oxidation reactions, respectively. The transfer coefficient α [eq 7] is, therefore, predicted to decrease linearly from 0.5 with increasing electrochemical driving force $\pm F(E - E^\circ)$. The derivation of eq 16 involves the assumption that the reactant and product free energy barriers are parabolic and have identical shapes, and that the reactions are adiabatic yet involve only a small "resonance splitting" of the free energy curves in the intersection region (21).

A number of experimental tests of eq 16 have been made for inorganic reactants (14, 22). Generally speaking, it has been found that, $\alpha \sim 0.5$ at small to moderate overpotentials, in agreement with eq 16. Tests of this relationship over sufficiently large ranges of overpotential, where the quadratic term becomes significant, are not numerous. A practical difficulty with multicharged redox couples is that the extent of the work term corrections is frequently sufficiently large to make the extraction of k_{corr}, and, hence, $\Delta G^{\ddagger}_e$ and α, from the observed

rate-potential behavior, fraught with uncertainty. However, we have recently obtained kinetic data for Cr^{2+}_{aq}, Eu^{2+}_{aq} and V^{2+}_{aq} electro-oxidation over wide ranges of anodic overpotential (up to 900 mv) under conditions where the electrostatic work terms are small (14). The anodic transfer coefficients, α_a, for all those reactions were found to decrease with increasing anodic overpotential, but to a greater extent than predicted by eq 16. This behavior contrasts that found for cathodic overpotentials, where the cathodic transfer coefficients α_c remain essentially constant at 0.5, even over regions of overpotential where detectable decreases in α_c are predicted by eq 16 (14, 23). These aquo redox couples, therefore, exhibit a markedly different overpotential dependence of the anodic and cathodic rate constants; this contrasts with the symmetrical dependence predicted by eq 16. An example of this behavior is shown in Figure 2 which is a plot of $\Delta G^{\ddagger}_e$ versus $(E - E^\circ)$ for $Cr^{3+/2+}_{aq}$ at the mercury-aqueous interface at both anodic and cathodic overpotentials. The solid curves are obtained from the experimental data and the dashed lines show the overpotential dependence of $\Delta G^{\ddagger}_e$ predicted from eq 16.

The prediction corresponding to eq 16 for driving force effects upon homogenous kinetics is (21)

$$\Delta G^{\ddagger}_{h,12} = \Delta G^{\ddagger}_{ih,12} + 0.5\ \Delta G^\circ_{12} + \frac{(\Delta G^\circ_{12})^2}{16\Delta G^{\ddagger}_{ih,12}} \qquad (17)$$

where $\Delta G^{\ddagger}_{ih,12}$ is the mean of the intrinsic barriers for the parent self-exchange reactions, $[0.5(\Delta G^{\ddagger}_{ih,1} + \Delta G^{\ddagger}_{ih,2})]$, and ΔG°_{12} is the free energy driving force for the cross reaction. Equation 17 has been found to be in satisfactory agreement with experimental data for a number of outer-sphere cross reactions having small or moderate driving forces. However, there appear to be significant discrepancies for some reactions having large driving forces (where the last term in eq 17 becomes important) in that the rate constants do not increase with increasing driving force to the extent predicted by eq 17; i.e., the values of $\Delta G^{\ddagger}_{h,12}$ are larger than those calculated from the corresponding values of $\Delta G^{\ddagger}_{ih,12}$ and ΔG°_{12} using eq 17 (15, 24-26).

It has been suggested that these apparent discrepancies could be due to the values of $\Delta G^{\ddagger}_{h,12}$ and $\Delta G^{\ddagger}_{ih,12}$ that are obtained from the experimental work-corrected rate constants being incorrectly large due to nonadiabatic pathways (24-26), or to the presence of additional unfavorable work terms arising from

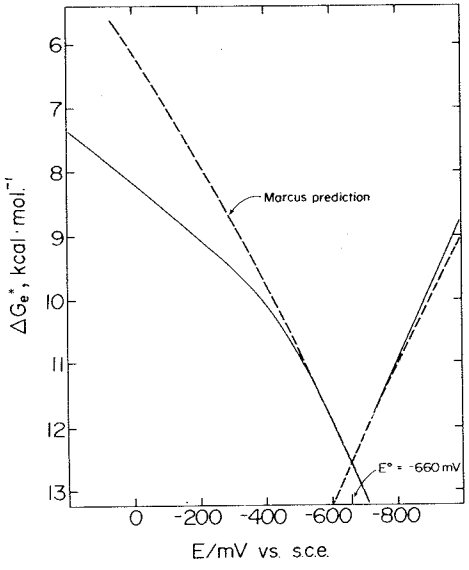

Figure 2. The electrochemical free energy of activation, ΔG_e^*, for $Cr(OH_2)_6^{3+/2+}$ at the mercury–aqueous interface, plotted against the electrode potential for both anodic and cathodic overpotentials. Solid lines are obtained from the experimental rate constant–overpotential plot in Ref. 14, using Eq. 6 (assuming $A = 5 \times 10^3$ cm·s^{-1}). Dashed lines are the predictions from Eq. 16.

the solvent orientation required to form the highly charged precursor complex (15). An alternative, or additional, explanation is that the free energy barriers are anharmonic so that the quadratic driving force dependence of eq 17 is inappropriate. It is interesting to note that the form of the discrepancies between the kinetic data for the electrooxidation of aquo cations and eq 16, and between the homogeneous rate data and eq 17, is at least qualitatively similar in that both involve unexpectedly small dependencies of the rate constants upon the thermodynamic driving force. Moreover, the large majority of homogeneous reactions for which such discrepancies have been observed involve the oxidation of aquo cations (15, 24). However, nonadiabaticity effects cannot explain the asymmetry between the (ΔG_e^* - E) plots at anodic and cathodic overpotentials (Figure 2). Also, any specific work term effects should be different (and probably smaller) at the mercury-aqueous interface compared with homogeneous reactions between multicharged cations (11); yet any anharmonicity of the free energy barriers should be similar, at least on the basis of the weak overlap model. A quantitative comparison of the driving force dependence of the kinetics of related electrochemical and homogeneous reactions should, therefore, shed light on the causes of the observed discrepancies for the latter, more complicated processes.

One can generally express the free energy barriers, ΔG_e^*, for the pair of cathodic and anodic electrochemical reactions 10a and 10b as [cf., eqs 7 and 16]:

$$\Delta G^*_{e,1} = \Delta G^*_{ie,1} + \alpha_1 \Delta G^\circ_1 \tag{18a}$$

and

$$\Delta G^*_{e,2} = \Delta G^*_{ie,2} + \alpha_2 \Delta G^\circ_2 \tag{18b}$$

where α_1 and α_2 are the transfer coefficients for these two reactions at a given electrode potential. A similar relationship may be written for the free energy barrier, $\Delta G^*_{h,12}$, of the corresponding homogeneous cross reaction (11) [cf., eq 17]:

$$\Delta G^*_{h,12} = \Delta G^*_{ih,12} + \alpha_{12} \Delta G^\circ_{12} \tag{19}$$

where α_{12} is a "chemical" transfer coefficient. Although α_1 and α_2 are determined only by the shapes of the free energy barriers for the individual redox couples at a given driving force, α_{12} is a composite quantity which is determined not only by both α_1

and α_2 but also by the relative magnitudes of $\Delta G^*_{ih,1}$, $\Delta G^*_{ih,2}$ and $\Delta G^*_{h,12}$.

Nevertheless, comparison of values of $\Delta G^*_{h,12}$ for a series of related cross reactions having systematically varying driving forces can yield useful information. Figure 3 is a plot of $\Delta G^*_{h,12}/\Delta G^*_{ih,12}$ versus $\Delta G^\circ_{12}/\Delta G^*_{ih,12}$ for a series of cross reactions involving the oxidation of various aquo complexes. (The values of ΔG^*_{12} and $\Delta G^*_{ih,12}$ were obtained from the measured homogeneous rate constants in the same way as the homogeneous free energies of activation given in Tables I and II. Details are given in ref. 15.) The graphical presentation in Figure 3 has the virtue that the values of $\Delta G^*_{h,12}$ for different cross reactions are normalized for variations in the intrinsic barriers $\Delta G^*_{ih,12}$; the driving force dependence of $\Delta G^*_{h,12}$ predicted by the Marcus model all fall on a common curve (shown as a solid line in Figure 3) when presented in this manner (27). [Omitted from Figure 3 are reactions involving $Co^{3+/2+}_{aq}$ since there is evidence that the measured self-exchange rate constant does not correspond to an outer-sphere pathway (28).] It is seen that the experimental points deviate systematically from the Marcus predictions in that the apparent values of α_{12} [eq 19] are significantly smaller than predicted from eq 17 at moderate to high driving forces. Figure 4 consists of the same plot as Figure 3 but for a number of outer-sphere cross reactions involving reductants other than aquo complexes (27). In contrast to Figure 3, reasonable agreement with the Marcus prediction is obtained (cf., ref. 27). The data in Figure 3 are also shown in Figure 5 as a plot of $[\Delta G^*_{12} - \Delta G^*_{i,12}]$ versus $-[0.5\Delta G^\circ_{12} + (\Delta G^\circ_{12})^2/16\Delta G^*_{i,12}]$. Since this plot is an expression of eq 17, the Marcus model predicts a slope of unity (the solid line in Figure 5). However, the experimental points (closed symbols) are almost uniformly clustered beneath this predicted line, and increasingly so as $-\Delta G^\circ_{12}$ increases, again indicating that α_{12} tends to be smaller than predicted.

It therefore seems feasible that these anomalously small values of α_{12}, noted from Figures 3 and 5, have their primary origin in the oxidation half-reactions which uniformly involve aquo complexes. This possibility was explored by converting the electrooxidation data into a form suitable for direct comparison with the homogeneous data in Figure 5 in the following manner. As noted above, the free energy barrier $\Delta G^*_{h,12}$ for each outer-sphere cross reaction will consist of contributions $\Delta G^*_{h,1}$ and

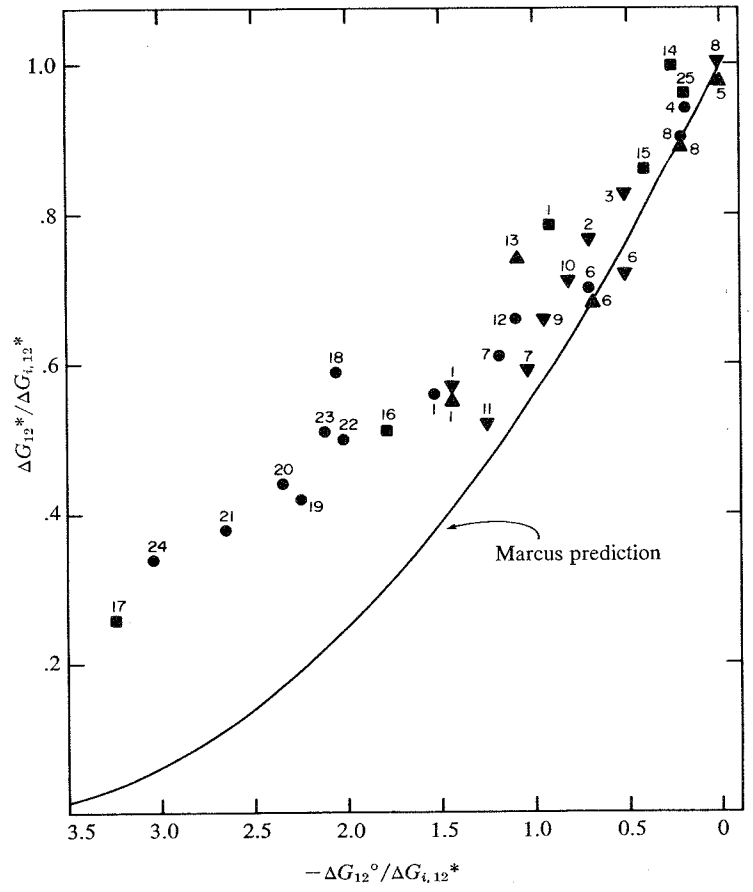

Figure 3. Plot of $\Delta G_{12}^*/\Delta G_{i,12}^*$ against $-\Delta G_{12}^\circ/\Delta G_{i,12}^*$ for homogeneous cross reactions involving oxidation of aquo cations. Reductants: ●, Eu_{aq}^{2+}; ▲, Cr_{aq}^{2+}; ▼, V_{aq}^{2+}; and ■, Ru_{aq}^{2+}. Key to oxidants and data sources: 1, Fe_{aq}^{3+}; 2, Ru_{aq}^{3+}; 3, Np_{aq}^{4+}; 4, V_{aq}^{3+}; 5, Eu_{aq}^{3+}; 6, $Ru(NH_3)_6^{3+}$; 7, $Ru(NH_3)_5py^{3+}$; 8, $Co(en)_3^{3+}$; 9, $Co(phen)_3^{3+}$; 10, $Co(bpy)_3^{3+}$ (1–10 are from Ref. 15); 11, $Ru(NH_3)_5isn^{3+}$ (Ref. 25); 12, $Co(phen)_3^{3+}$ (Ref. 24); 13, $Co(phen)_3^{3+}$ (Ref. 32); 14 to 17 and 25 are from Ref. 33: 14, $Co(phen)_3^{3+}$; 15, $Ru(NH_3)_5isn^{3+}$; 16, $Os(bpy)_3^{3+}$; 17, $Ru(bpy)_3^{3+}$; 18 to 22 are from Ref. 34: 18, $*Ru[4,4'(CH_3)_2bpy]_3^{2+}$; 19, $*Ru(phen)_3^{2+}$; 20, $*Ru(bpy)_3^{2+}$; 21, $*Ru(5\text{-Cl phen})_3^{2+}$; 22, $*Ru[4,7\text{-}(CH_3)_2phen]_3^{2+}$; 23, $*Os(5\text{-Cl phen})_3^{2+}$ (Ref. 35); 24, $Ru[4,7\text{-}(CH_3)_2phen]_3^{3+}$ (Ref. 36); 25, $Ru(NH_3)_5py^{3+}$. An asterisk (*) indicates the oxidant is a photoexcited state reactant.

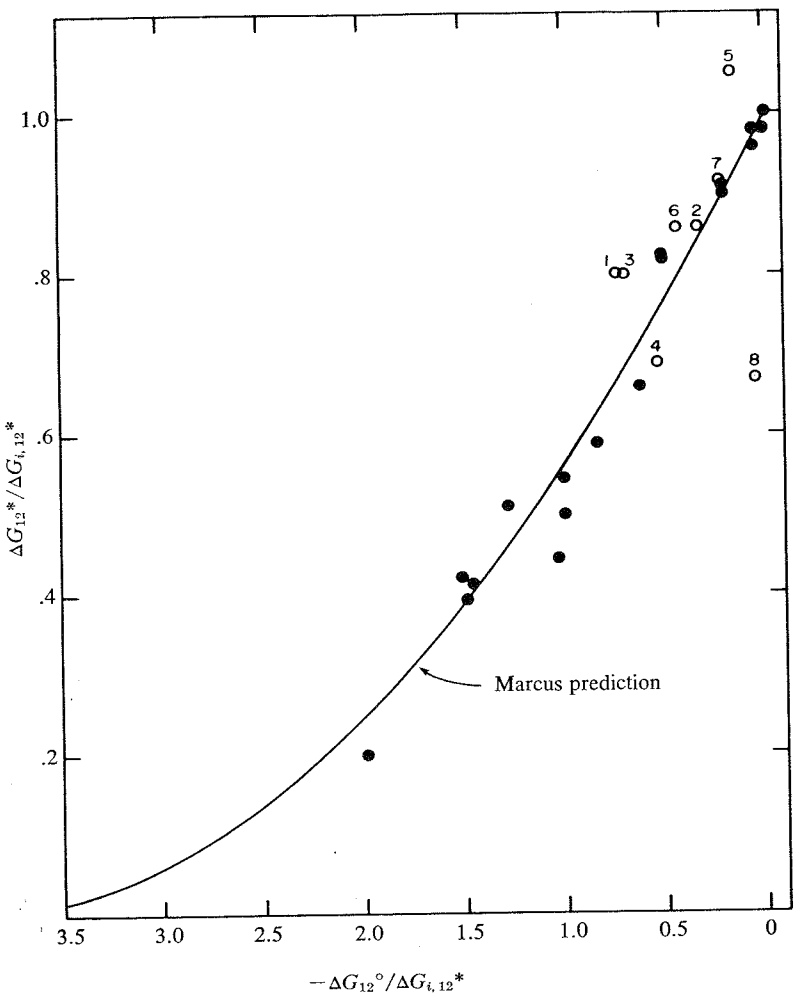

Figure 4. Plot as for Figure 3, but involving reductants other than aquo complexes. Key to reactions and data sources: ●, Co(III)/(II) macrocycle oxidants (data are given in Figures 2, 5, 6, and Ref. 27); ○, other nonaquo oxidants; 1, $Ru(NH_3)_5py^{3+}$ + $Ru(NH_3)_6^{2+}$; 2, Ru_{aq}^{3+} + $Ru(NH_3)_6^{2+}$; 3, $Co(phen)_3^{3+}$ + $Ru(NH_3)_6^{2+}$; 4, $Co(bpy)_3^{3+}$ + $Ru(NH_3)_6^{2+}$; 5, $Co(phen)_3^{3+}$ + $Ru(NH_3)_5py^{2+}$ (1–N from Ref. 15); 6, horse heart ferricytochrome c + $Ru(NH_3)_6^{2+}$ (Ref. 37); 7, $Co(phen)_3^{3+}$ + horse heart ferrocytochrome c (Ref. 38); 8, $Ru(NH_3)_4bpy^{3+}$ + $Ru(NH_3)_5py^{2+}$ (Ref. 24).

$\Delta G^*_{h,2}$ from the oxidant and reductant, respectively. In the "weak overlap" limit, $\Delta G^*_{h,1}$ and $\Delta G^*_{h,2}$ will equal the free energy barriers $\Delta G^*_{e,1}$ and $\Delta G^*_{e,2}$ for the corresponding electrochemical reactions at an electrode potential where the sum ($\Delta G^*_{e,1}$ + $\Delta G^*_{e,2}$) is a minimum [eq 12 and Figure 1]. Estimates of $\Delta G^*_{h,2}$ for Eu^{2+}_{aq}, Cr^{2+}_{aq}, and V^{2+}_{aq} oxidation as a function of the half-reaction driving force ΔG°_2 [= $-F(E - E^\circ_2)$] were obtained from the corresponding (ΔG^*_e - E) plots (see Figure 2 and ref. 14) by assuming that they have the same shape but replacing the value of ΔG^*_e at $\Delta G^\circ_2 = 0$ (i.e., ΔG^*_{ie}) by 0.5 ΔG^*_{ih}. [This procedure corrects for any differences between ΔG^*_{ie} and $0.5\Delta G^*_{ih}$ (Table II) resulting from the limitations of the weak overlap model (eq 14)]. The accompanying plots of $\Delta G^*_{h,1}$ versus ΔG°_1 for the reduction half reactions involved in Figure 5 were constructed using the experimental value of $\Delta G^*_{ih,12}$ by assuming that the harmonic oscillator model applies, i.e., by utilizing eq 16 written for homogeneous half reactions:

$$\Delta G^*_{h,1} = 0.5\ \Delta G^*_{ih,12} + 0.5\ \Delta G^\circ_1 + (\Delta G^\circ_1)^2/8\ \Delta G^*_{ih,12} \qquad (20)$$

These pairs of ($\Delta G^*_{h,1}$ - ΔG°_1) and ($\Delta G^*_{h,2}$ - ΔG°_2) curves were plotted on a common driving force (i.e., electrode potential) axis such that (ΔG°_1 - ΔG°_2) = ΔG°_{12}, and the required estimates of $\Delta G^*_{h,12}$ for each cross reaction were then obtained from the sum ($\Delta G^\circ_{h,1}$ + $\Delta G^\circ_{h,2}$) at the value of ΔG° where the quantity has a minimum value [eq 12]. These estimates of $\Delta G^*_{h,12}$ are plotted as open symbols in Figure 5 for the reactions having moderate to large driving forces ($-\Delta G^\circ_{12}$ > 8 kcal mol^{-1}), alongside the corresponding experimental values of $\Delta G^*_{h,12}$ (closed symbols). It is seen that the "electrochemical" estimates of values of $\Delta G^*_{h,12}$ diverge from the straight line predicted from the harmonic oscillator model to a similar, albeit slightly smaller, extent than the experimental values. Admittedly, there is no particular justification for assuming that the reduction half reactions obey the harmonic oscillator model. However, it turns out that the estimates of $\Delta G^*_{h,12}$ are relatively insensitive to alterations in the shapes of the ($\Delta G^*_{h,1}$ - ΔG°_1) plots.

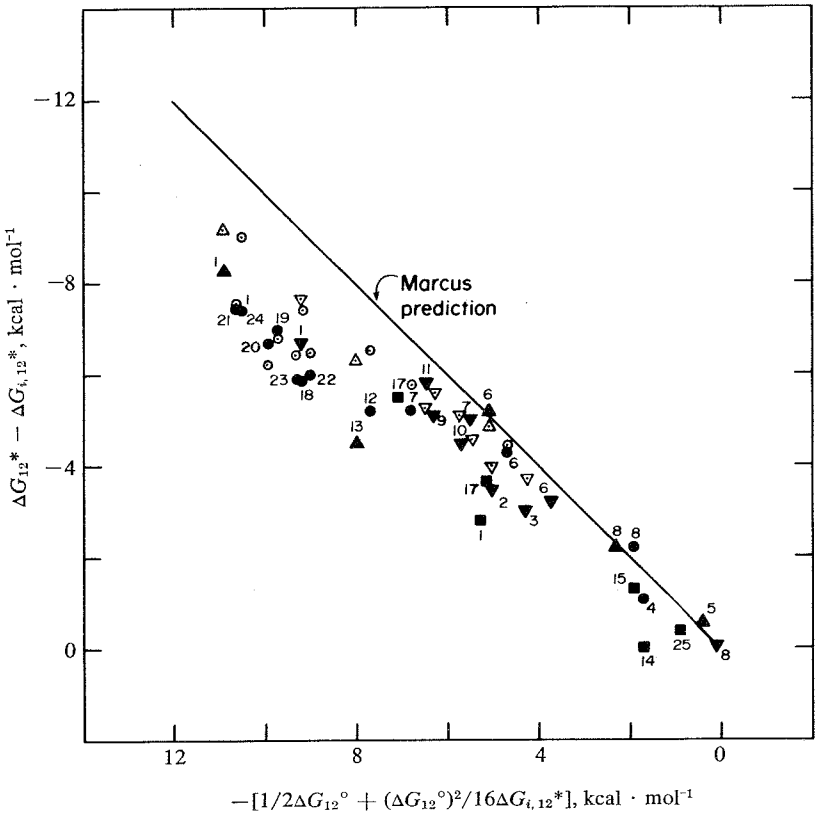

Figure 5. Plot of $(\Delta G_{12}^* - \Delta G_{i,12}^*)$ *for homogeneous cross-reactions involving oxidation of aquo complexes given in Figure 3, against the thermodynamic driving force function* $-[0.5\Delta G_{12}^\circ + (\Delta G_{12}^\circ)^2/16\Delta G_{i,12}^*]$. *Closed symbols are obtained from homogeneous data; key to points as in Figure 3. Open symbols are corresponding points obtained from electrochemical kinetic data for oxidation of aquo cations. Reductants:* ○ *and* ●, Eu_{aq}^{2+}; △ *and* ▲, Cr_{aq}^{2+}; ▽ *and* ▼, V_{aq}^{2+}; *and* ■, Ru_{aq}^{2+}.

It therefore seems reasonable that the deviations of the activation free energies for highly exoergic electrochemical and homogeneous reactions, illustrated in Figures 2 and 5, may arise partly from the same source, i.e., from values of α_2 for the oxidation half reactions that are unexpectedly small.[2] That is not to say that other factors are not responsible, at least in part, for these discrepancies. Nonadiabaticity, work terms, specific solvation, and other environmental effects may all play important roles depending on the reactants. For example, there is evidence to suggest that the true rate constant for outer-sphere $Fe_{aq}^{3+/2+}$ self-exchange is significantly smaller than the directly measured value (29); this can account for a good part of the unexpectedly slow rates of cross reactions involving this couple.

It remains to consider possible reasons for these apparent deficiencies of the harmonic oscillator model for the oxidation of aquo cations. Some discussion of the electrochemical results has been given previously (14). It was concluded that the most likely explanation for the observed disparities between the experimental results and the predictions of eq 16 (Figure 2) is that the reactant and product free energy barriers for the aquo redox couples have markedly different shapes. Such an asymmetry of the free energy barriers is unlikely to arise from inner-shell (metal-ligand vibrational) contributions, at least within the confines of a classical model. Thus, choosing even unreasonably large differences in vibrational force constants for the oxidized and reduced forms generates much smaller differences in the shapes of the resulting anodic and cathodic Tafel plots than are observed experimentally (Figure 2; also see 14). Indeed, such calculations performed for homogeneous reactions led to an earlier assertion that anharmonicity effects were unlikely to account for the extent of the observed breakdowns in the applicability of the Marcus cross relationship [eq 17] as exemplified in Figures 3 and 5 (24). A plausible, albeit somewhat inaccessible, source of asymmetry in the free energy barriers could lie in major differences in short-range solvent structure between the reduced and oxidized aquo complexes. There is strong evidence that tripositive aquo complexes induce extensive solvent ordering via field-assisted hydrogen bonding with the aquo ligands, which is partly dissipated upon reduction to the dipositive species (9, 30). This short-range reorientation of water molecules may well contribute unequally to the individual free energy curves for the oxidized and reduced species, thereby generating the required nonsymmetry. A related point is that the reactant and product potential-energy barriers will be highly nonsymmetrical even when the free-energy driving force, ΔG_{rc}°, is zero (i.e., at E°), as a result of the especially large positive values of ΔS_{rc}° for the aquo redox couples (Table I). Thus,

the electrooxidation reactions will be highly exothermic ($-\Delta H^\circ_{rc} \simeq 15$ kcal mol^{-1}) even when $\Delta G^\circ_{rc} = 0$, and increasingly so at anodic overpotentials. In contrast, the electroreduction reactions are endothermic ($\Delta H^\circ_{rc} > 0$) within the entire overpotential range that is accessible to experiment.

Conclusions

It seems clear that kinetic as well as thermodynamic data gathered for simple electrode reactions can contribute significantly towards the development of our fundamental understanding of electron transfer in condensed media. In particular, detailed studies of electrochemical kinetics, with due regard for work term corrections, can yield information on the shapes of free energy barriers, and also their enthalpic and entropic components, that are largely inaccessible from studies of homogeneous redox kinetics. The former can provide a direct means of detecting deficiencies in the applicability of the harmonic oscillator model which forms the kernel of most contemporary treatments of electron transfer.

Experimental comparisons between the kinetics of related electrochemical and homogeneous reactions in suitable cases can also yield insights into the differences, as well as similarities, between these two major types of redox processes (3, 11, 31). Unfortunately, there is still a paucity of electrochemical kinetic data on substrates other than mercury. However, recent advances in the methods for preparing and characterizing clean metal surfaces, particularly for single crystals, should allow the acquisition of quantitative data for a much wider range of reactions and surface environments than hitherto available. It is hoped that a greater comparison of results for heterogeneous and homogeneous processes will occur in the future; this should be to the benefit of both areas.

Acknowledgements

We are grateful to Prof. John Endicott for sending us a copy of ref. 28 prior to publication. This work is supported in part by the Air Force Office of Scientific Research and the Office of Naval Research.

Literature Cited

1. Marcus, R. A. J. Phys. Chem. 1968, 72, 891.
2. Sutin, N. Acct. Chem. Res. 1968, 1, 225.
3. Weaver, M. J. Inorg. Chem. 1979, 18, 402.
4. Parsons, R. Croat. Chim. Acta 1970, 42, 281.
5. Temkin, M. Zh. Fiz. Khim. 1948, 22, 1081.

6. Weaver, M. J. J. Phys. Chem. 1976, 80, 2645.
7. Weaver, M. J. Israel J. Chem. 1979, 18, 35.
8. Weaver, M. J. J. Phys. Chem. 1979, 83, 1748.
9. Yee, E. L.; Cave, R. J.; Guyer, K. L.; Tyma, P. D.; Weaver, M. J. J. Am. Chem. Soc. 1979, 101, 1131.
10. Newton, T. W. J. Chem. Educ. 1968, 45, 571.
11. Weaver, M. J. J. Phys. Chem. 1980, 84, 568.
12. Weaver, M. J. Inorg. Chem. 1976, 15, 1733.
13. Marcus, R. A. J. Phys. Chem. 1963, 67, 853.
14. Tyma, P. D.; Weaver, M. J. J. Electroanal. Chem. 1980, 111, 195.
15. Weaver, M. J.; Yee, E. L. Inorg. Chem. 1980, 19, 1936.
16. Weaver, M. J.; Satterberg, T. L. J. Phys. Chem. 1977, 81, 1772.
17. Brunschwig, B. S.; Logan, J.; Newton, M. D.; Sutin, N. J. Am. Chem. Soc. 1980, 102, 5798.
18. Endicott, J. F.; Schroeder, R. R.; Chidester, D. H.; Ferrier, D. R. J. Phys. Chem. 1973, 77, 2579.
19. Saji, T.; Yamada, T.; Aoyagui, S. J. Electroanal. Chem. 1975, 61, 147.
20. Saji, T.; Mariyama, Y.; Aoyagui, S. J. Electroanal. Chem. 1978, 86, 219.
21. Marcus, R. A. J. Chem. Phys. 1965, 43, 679.
22. See ref. 14 for references to earlier work.
23. Weaver, M. J.; Anson, F. C. J. Phys. Chem. 1976, 80, 1861.
24. Chou, M.; Creutz, C.; Sutin, N. J. Am.Chem. Soc. 1977, 99, 5615.
25. Brown, G. M.; Krentzien, H. J.; Abe, M.; Taube, H. Inorg. Chem. 1979, 18, 3374.
26. Balzani, V.; Scandola, F.; Orlandi, G.; Sabbatini, N.; Indelli, M. T. J. Am. Chem. Soc. 1981, 103, 3370.
27. Endicott, J. F.; Durham, B.; Glick, M. D.; Anderson, T. J.; Kuszaj, J. M.; Schmonsees, W. G.; Balakrishnan, K. P. J. Am.Chem. Soc. 1981, 103, 1431.
28. Endicott, J. F.; Durham, B.; Kumar, K. Inorg. Chem. in press.
29. Hupp, J. T.; Weaver, M. J., to be submitted for publication.
30. Weaver, M. J.; Nettles, S. M. Inorg. Chem. 1980, 19, 1641.
31. For example, see Guyer, K. L.; Barr, S. W.; Cave, R. J.; Weaver, M. J., in "Proc. 3rd Symp. on Electrode Processes", Bruckenstein, S.; McIntyre, J. D. E.; Miller, B.; Yeager, E., Eds., Electrochemical Society: Princeton, NJ, 1980; p. 390.

32. Przystas, T.J.; Sutin, N. J. Am. Chem. Soc. 1973, 95, 5545.
33. Böttcher, W; Brown, G.M.; Sutin, N. Inorg. Chem. 1979, 18, 1447
34. Creutz, C. Inorg. Chem. 1978, 17, 1056.
35. Creutz, C.; Chow, M.; Netzel, T.L.; Okumura, M.; Sutin, N. J. Am. Chem. Soc. 1980, 102, 1309.
36. Lin, C.-T.; Böttcher, W.; Brown, G.M.; Creutz, C.; Sutin, N. J. Am. Chem. Soc. 1976, 98, 6536
37. Ewall, R.X.; Bennett, L.E. J. Am. Chem. Soc. 1974, 96, 940.
38. McArdle, J.V.; Gray, H.B.; Creutz, C.; Sutin, N. J. Am. Chem. Soc. 1974, 96, 5737.

RECEIVED April 21, 1982.

General Discussion—Some Comparisons Between the Energetics of Electrochemical and Homogeneous Electron-Transfer Reactions

Leader: Stephen Isied

DR. NOEL HUSH (University of Sydney): On the question of the correlation between the free energy of activation for the homogeneous and the heterogeneous processes (e.g., $Fe^{3+,2+}$), some years ago I suggested that there is probably an important difference between these processes [Hush, N. S. Electrochim. Acta 1968, 13, 1004]. If one uses the model in which there is an outer-sphere contribution arising from the interaction with the dielectric and an inner-shell contribution due to vibrational modes, then it is reasonable to suppose that the inner-shell contribution for the homogeneous process will be twice that for the corresponding heterogeneous reaction. However, such a relationship need not necessarily hold for the remaining terms. When we bring two ions together to separation R in the homogeneous case, we have a term proportional to -1/R in the free energy of activiation, which reduces the dielectric interaction energy. But in the case of reaction at a metallic electrode, an analogous term will be present only if there is an appreciable image effect.

My conclusion (based on double-layer theory) was that, under the usual experimental conditions, the image term is almost entirely screened off. When this is so, the dielectric contribution to the activation free energy is essentially the same for the homogeneous and the heterogeneous process.

A number of years ago, John Hale made calculations of the free energies of activation for transfers at metallic electrodes using that assumption, and obtained quite reasonable agreement with experiment [Hale, J. M., in "Reactions of Molecules at Electrodes," Hush, N. S., Ed.; Wiley-Interscience: New York, N.Y., 1971; Chapter 4]. So if that is the case, one would not expect to get a 1:2 heterogeneous:homogeneous ratio when the dielectric term was particularly small. This may arise for certain classes of molecules in which the dominant terms are the inner-shell ones. But for the small aquo ions, for example, one might well expect the ratio of reorganizational energy parameters to differ from 1:2. Of course, a detailed calculation may suggest some small contribution from image effects under the usual experimental conditions of reasonably high ionic strength, but I do not think that this has yet been domonstrated.

DR. WEAVER: As I have shown in Tables I and II of my contribution, the activation free energies, and especially the activation enthalpies, for electrochemical exchange of aquo cations are significantly greater than one-half the corresponding activation energies of the homogeneous self-exchange reactions. This is qualitatively in accord with the model you cited which asserts that there is no imaging in the electrochemical case.

Nevertheless, I think imaging remains significant because there is no way that the image in a transition state can be entirely screened by surrounding ions. One is, in a sense, getting two transition states because of the Franck-Condon barrier, and there is no way that the surrounding ions can entirely screen both the reactant and product transition states at the same time. Also, as I have pointed out in my presentation and in reference 11, the activation energy for the outer-sphere electrochemical exchange is generally expected to be greater than one-half of the homogeneous activation energy even on the basis of the imaging model since the presence of the inner layer of solvent molecules will make the distance between the reacting ion and its image in the electrode greater than the contact distance between the reacting ions in homogeneous solution.

DR. HUSH: There is thought to be a mystery as to why the $Eu^{3+,2+}$ self-exchange is so slow in aqueous solution. I believe the reason is very simple. The coordination number and symmetry of the water molecules in the first shell around the two aquo ions is completely different so the electron-exchange reaction is inhibited by the slow rate of dissociating a water molecule and reorganizing the inner-coordination sphere. It is quite unnecessary, I believe, to invoke possible electronic nonadiabaticity to account for the observed slow kinetics.

In the electrochemical case, this ought to be reflected both in slow exhange kinetics and also in a value of the transfer coefficient significantly different from one-half. Dr. Vlcek originally attributed the observed slow electrochemical rate to transfer via excited electronic states. I do not think that is correct. I believe that slow kinetics of ligand exchange in the first solvation shells are generally responsible for the unusual features of the $Eu^{3+,2+}$ exchange rates.

We carried out some measurements some years ago in order to measure the transfer coefficient in DMF for this couple at a mercury electrode [Hush, N. S.; Dyke, J. M. J. Electroanal. Interfac. Electrochem. 1974, 53, 253]. The deviation from one-half for the value so obtained was consistent with reasonable values for the free energy of activation of ligand exchange in the inner-coordination spheres.

Thus, in my opinion, nonadiabaticity does not have to be invoked to explain the slow homogeneous and heterogeneous $Eu^{3+,2+}$ exchange rates.

DR. WEAVER: I agree that the difference in coordination numbers between Eu^{3+} and Eu^{2+} could contribute importantly to the observed slow rates of electron transfer. However, it is true to say, from our data, anyway, that the way in which the

alpha for the $Eu^{3+,2+}$ couple depends upon the overpotential in aqueous media is very similar to the behavior of the $Cr^{3+,2+}$ and the $V^{3+,2+}$ couples as well.

DR. HUSH: The work of Anson showed that Parsons' and Passeron's experiments [Parsons. R.; Passeron, E. J. Electroanal. Chem. 1966, 12, 524] on the dependence of alpha for $Cr^{3+,2+}$ upon potential were incorrect [Anson, F. C.; Rathjen, N.; Frisbee, R. D. J. Electrochem. Soc. 1970, 117, 477].

DR. WEAVER: Anson only looked at the cathodic side which yields very little change in alpha with overpotential. The anodic side, as I showed, exhibits a very marked dependence of alpha on overpotential.

DR. HENRY TAUBE (Stanford University): Though I agree that present evidence points to the conclusion that the slow rate for the aquo $Eu^{3+,2+}$ exchange is attributable to differences in solvation between the two oxidation states, I still find it very puzzling that these differences are greater for this system than for aquo $Fe^{3+,2+}$ where the radii are much smaller. When an ion gets large enough, specific solvation must lose its meaning. For Cs^{+}, I imagine there are many solvent configurations about the metal ion which have approximately the same energy.

DR. WEAVER: With regard to the assignment of the very slow exchange rate for aquo $Eu^{3+,2+}$ to nonadiabaticity or to solvational rearrangement, we find that encapsulation of europium inside a 2.2.1- or 2.2.2-cryptand, forming a macrobicyclic ligand shell around the ion, results in homogeneous self-exchange rates approaching 10 $M^{-1}s^{-1}$ in contrast to $\sim 10^{-5}$ $M^{-1}s^{-1}$ for aquo $Eu^{3+,2+}$ [Yee, E. L.; Weaver, M. J., unpublished results]. We don't believe that those results can be easily explained by electron tunneling since the f-orbital overlap is likely to be smaller for the europium cryptate couple.

DR. DAVID RORABACHER (Wayne State University): We have recently obtained very similar results for the $Cu^{2+,+}$ couple. This is one of the classic redox couples involving a large change in coordination number, Cu(II) preferring a tetragonal geometry while Cu(I) is predominantly tetrahedral. For aquo $Cu^{2+,+}$, we have recently estimated that the self-exchange rate constant at 25 C is $\sim 2 \times 10^{-6}$ $M^{-1}s^{-1}$. When complexed with macrocyclic tetrathiaether (S_4) ligands, however, the self-ex-

change rate constant increases by about eight orders of magnitude to $\sim 10^2$ $M^{-1}s^{-1}$ [Martin, M. J.; Koenigbauer, M. J.; Endicott, J. F.; Rorabacher, D. B., unpublished results]. When a macrocyclic pentathiaether (S_5) ligand is used, the self-exchange rate constant increases further to $\sim 10^4$ $M^{-1}s^{-1}$.

We believe that these large changes in rate constant are primarily attributable to restrictions imposed upon the inner-coordination sphere by the macrocyclic ligands. Presumably, the use of a suitable macrobicyclic ligand, such as you have used with europium, would induce even larger changes in the $Cu^{2+,+}$ self-exchange rate constant. We are planning to pursue such studies in the near future.

DR. EPHRAIM BUHKS (University of Delaware): Is there any experimental evidence indicating the possibility of electron transfer from the electrode into the excited electronic state of a transition metal ion?

DR. WEAVER: Such a process is possible but I don't know of any data which would provide direct evidence. At metal surfaces, at least, excited electronic states of nearby reacting ions might be expected to be quenched rapidly. Semiconductor surfaces would provide more systems with which to search for such an effect.

DR. ALBERT HAIM (State University of New York at Stony Brook): When you vary the free energy of reactions and go to very exoergonic reactions, you enter into a region which is sometimes called the inverted region or the abnormal region. Has anything similar been observed in very highly exoergonic reactions in electrochemical reductions or oxidations?

DR. WEAVER: The major problem seems to be that when we talk about a fast reaction in electrode kinetics, with rate constants in the range 0.1 - 10 cm s^{-1}, we are referring to a process which has an activation energy equivalent to a homogeneous reaction having a rate constant about 10^5 $M^{-1}s^{-1}$. We are not able to explore such a large range of rate constants and, hence, driving force in electrochemical processes because diffusion becomes the overall rate-limiting step at much smaller rates than occurs in homogeneous solution, two-dimensional diffusion being much less efficient than three-dimensional diffusion. Therefore, it is extremely difficult to measure rate constants that correspond to a sufficiently small activation barrier to investigate the predicted onset of inversion.